Chemical Modification of Fluorinated Polyimides: New Thermally Curing Hybrid Polymers with POSS

Michael E. Wright,*,† Brian J. Petteys,† Andrew J. Guenthner,† Stephen Fallis,† Gregory R. Yandek,† Sandra J. Tomczak,‡ Timothy K. Minton,§ and Amy Brunsvold§

Research & Engineering Sciences Department, Chemistry Division, NAVAIR−US NAVY, China Lake, California 93555-6100; Propulsion Materials Application Branch, Air Force Research Laboratory, Edwards AFB, California 93524; and Department of Chemistry and Biochemistry, Montana State University, Bozeman, Montana 59717

Received February 20, 2006; Revised Manuscript Received May 9, 2006

ABSTRACT: A series of four new end-capped and hydroxymethyl-functionalized polyimides were prepared. Through a two-step chemical modification process (3-aminopropyl)(hepta-*i*-butyl) polyhedral oligomeric silsesquioxane (POSS) was covalently attached to the polymer backbone. POSS loading levels as high as 36 wt % could be obtained while maintaining excellent processability and optical clarity of thin films. Concurrent attachment of either a cyanate ester or hydroxyethyl methacrylate (HEMA) group afforded processable POSS-polyimides that underwent thermal curing to yield solvent-resistant films, both having final T_g's of 251 °C. Kinetic analysis of the cure reactions yielded energy of activations of 93 kJ/mol (cyanate ester) and 103 kJ/mol (HEMA). Exposure of a POSS-polyimide containing ∼31 wt % POSS to atomic oxygen displayed no measurable level of erosion relative to a Kapton H standard.

Introduction

Polyhedral oligomeric silsesquioxanes (POSS) are a family of nanoscale inorganic cage structures containing a silicon/oxygen framework that are a intermediate ($RSiO_{1.5}$) between silica (SiO_2) and silicone (R_2SiO).[1,2] The vast majority of commercially available POSS compounds consist of a Si_8O_{12} cage functionalized at one corner (i.e., Si atom) with an organic substituent that provides a point for synthetic elaboration (Figure 1).[3] It is this combination of an inorganic core and a hydrocarbon periphery that imparts unique physical and chemical properties to POSS compounds.

Over the past decade there has been a steadily increasing interest in the creation of POSS-based structures for use as blocks in nanocomposite structures for a variety of applications.[4] As mentioned above, a tremendous amount of polymer-based POSS nanocomposites has been created based on POSS cages functionalized at one silicon atom, and in some cases control over long-range ordering can be achieved.[5] Very recently, it was shown that very selective opening of the POSS cage can be achieved to afford difunctional POSS monomers, and these can be incorporated into polymeric materials.[6] Finally, there exist several examples of POSS molecules that carry reactive functionality at each silicon atom, and these have found widespread use in creating new nanocomposite architectures[7] with interesting physical/mechanical[8] and optical properties.[9]

One area in particular that POSS has shown outstanding performance is the ability to impart resistance toward chemical degradation by atomic oxygen (AO).[10] Atomic oxygen comprises up to 90% of the low earth orbit (LEO) environment and is known to promote rapid chemical degradation of all organic polymeric coatings that include Kapton H. Exposure of a variety of POSS-containing polymers to simulated LEO environmental conditions has shown that these materials possess dramatically improved resistance to chemical degradation by the highly reactive AO.[11] This type of adaptive feature is attributed to an oxidative degradation of the POSS cage to create a protective layer of silica {i.e., $(SiO_2)_n$} that minimizes further degradation by AO. Thus, POSS-containing polymers hold great promise for extending the lifetime of organic materials that must function for long periods of time in the LEO environment.

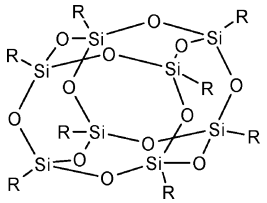

Figure 1. Structural representation of POSS nanoparticle Si_8O_{12} cage where R = alkyl, aryl, etc.

As part of an ongoing examination into new space survivable materials, we present herein a method of covalently attaching POSS at very high wt % loadings to a variety of polyimide backbone structures. The new POSS-modified polyimides are easily processed into optically clear films by spin-casting, doctor-blading, or aerosol spray techniques. Furthermore, we demonstrate that by incorporation of a cross-linking moiety the films can be thermally cured into solvent-resistant coatings that retain their optical clarity. Last, we present exposure data for one polyimide coating that contained ∼31 wt % of POSS. The material exhibits excellent resistance (∼0% degradation relative to Kapton H) to atomic oxygen (simulated LEO), and these new polyimides are much more transparent in the visible region than Kapton H.

Results and Discussion

Hydroxymethyl-Functionalized Polyimide Synthesis. Recently, we reported the synthesis of a new benzyl alcohol diamine, 3,5-bis(4-aminophenoxy)-1-hydroxymethylbenzene (BHB), and that it can be readily copolymerized with 4,4′-

† NAVAIR-US NAVY.
‡ Air Force Research Laboratory.
§ Montana State University.

10.1021/ma060372d CCC: $33.50
Published on Web 06/17/2006

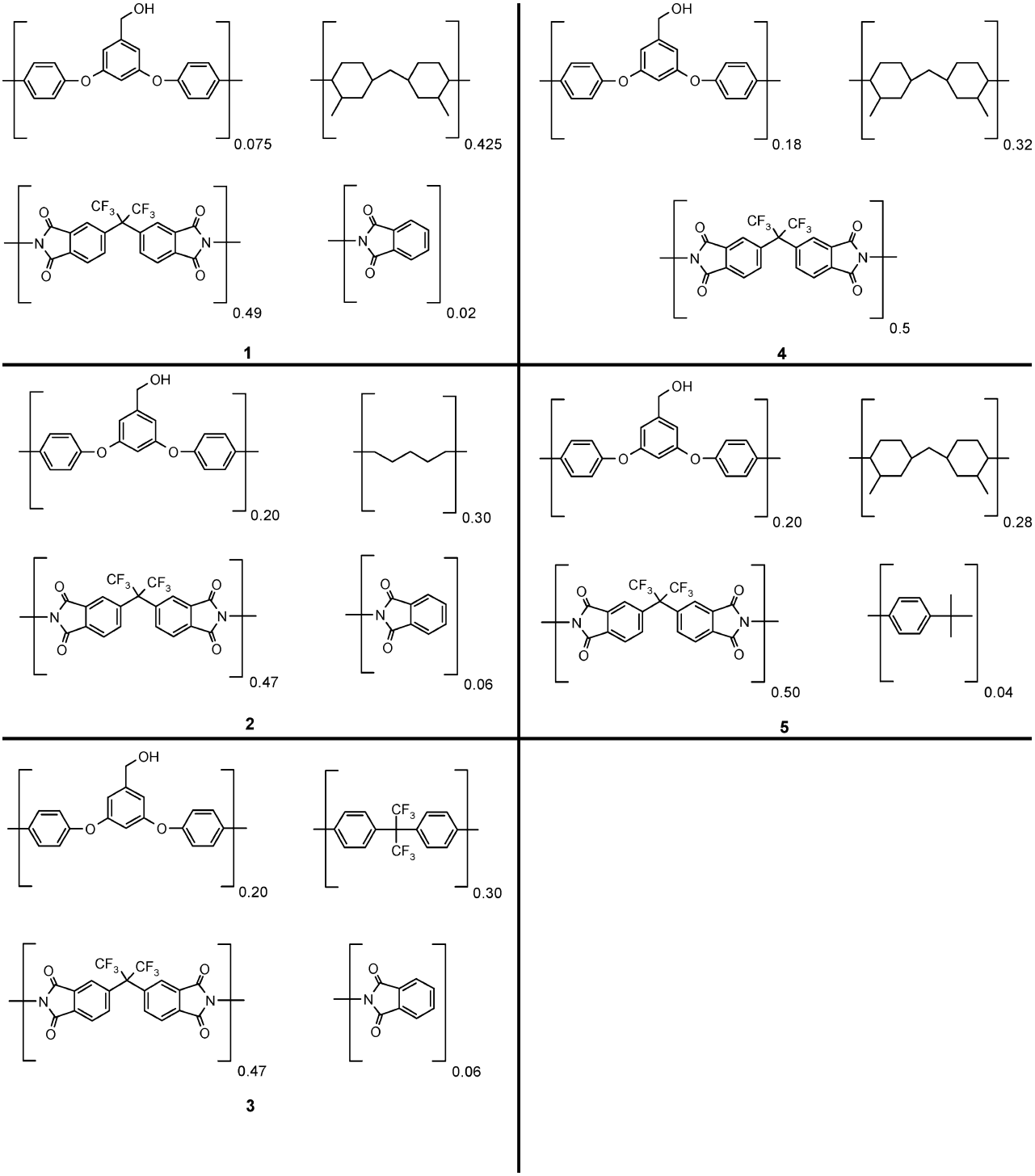

Figure 2. Chemical structures of polyimides **1**−**5** containing the hydroxymethyl reactive subunit BHB.

(hexafluoroisopropylidene)diphthalic anhydride (6-FDA) to afford a new hydroxymethyl-functionalized polyimide.[12] Our initial work included 2,2-bis(4-aminophenyl)hexafluoropropane (6-F diamine) as a comonomer to dilute the hydroxymethyl sites in the polymer backbone. We have now extended this work to include two hydrocarbon alkyl diamines, 1,5-diaminopentane and 2,2′-dimethyl-4,4′-methylenebis(cyclohexylamine) (RF-24) (Figure 2, Table 1). In each case the copolymers appear to be random and display a T_g that reflects the structural stiffness of the codiamine. To control molecular weight of the hydroxyl-functionalized polyimides, we added phthalic anhydride or 4-*tert*-butylaniline as end-caps. We have characterized polyimides **1**−**5** by ^{1}H and ^{13}C NMR spectroscopy, differential scanning calorimetry (DSC), thermogravimetric analysis (TGA), and size exclusion chromatography (SEC).

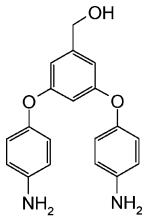

BHB

Table 1. Hydroxymethyl-Functionalized Polymer Compositions

	monomer content (mol %)[a]								
polymer	6-FDA	PhthAn	*t*-BuAn	Cad	CF6	RF-24	BHB	mequiv OH	T_g (°C)
1	49	2				42	8	0.23	260
2	47	6		30			20	0.68	196
3	47	6			30		20	0.55	279
4	50					32	18	0.53	279
5	50		4			28	20	0.59	267

[a] Abbreviations: 6-FDA = 4,4′-(hexafluoroisopropylidene)diphthalic anhydride; PhthAn = phthalic anhydride; *t*-BuAn = *tert*-butylaniline; Cad = 1,5-diaminopentane; CF6 = 2,2-bis(4-aminophenyl)hexafluoropropane; RF-24 = 2,2′-dimethyl-4,4′-methylenebis(cyclohexylamine); BHB = 3,5-bis(4-aminophenoxy)-1-hydroxymethylbenzene.

The presence of the hydroxymethyl moiety as a reactive subunit within the polymer backbone can be introduced at a variety of stoichiometric levels. All work to date indicates that the feed ratio of BHB matches that found in the polyimide and that all the hydroxymethyl sites are available for attachment chemistry. Table 1 also includes a listing for the mequiv of hydroxymethyl sites available per gram of each functionalized polyimide.

Polymer Modification. The reactive $-CH_2OH$ subunits of polyimides **1**−**4** are first functionalized by treatment with excess adipoyl chloride in the presence of 2,6-di-*tert*-butyl-4-methylpyridine and 4-(dimethylamino)pyridine (DMAP). This polymer is isolated by precipitation into ether, collected, washed, and briefly dried under reduced pressure to afford a new polyimide with a highly reactive pendant acid chloride functional group (Scheme 1). Redissolving the latter polymers in dichloromethane followed by treatment with 3-aminopropylisobutyl-POSS in the presence of DMAP affords the POSS-modified polymers **6**−**9** (from polymers **1**−**4**, respectively). Isolation is accomplished by precipitation into methanol, followed by collection of the polymer on a glass frit, and then drying at reduced pressure. Analysis of the materials by ^{1}H NMR spectroscopy is consistent with a high efficiency (>95%) attachment of the POSS moiety in each example. More specifically, we find in the ^{1}H NMR spectra a 1:1 integration ratio for the benzylic-CH_2 and the C_3 methylene (i.e., *CH*$_2$-NHCO) POSS propyl signals. This latter result is consistent with complete side chain attachment. Furthermore, the C_3 methylene of the POSS propylene chain displays an expected downfield shift of $\delta \sim 0.5$ ppm as a consequence in going from an amino group to the chemically attached amide. On the basis of the spectroscopic data the calculated Si_8O_{12} content of the POSS-modified polymers **6**, **7**, **8**, and **9** are 8, 17, 15, and 15 wt %, respectively.

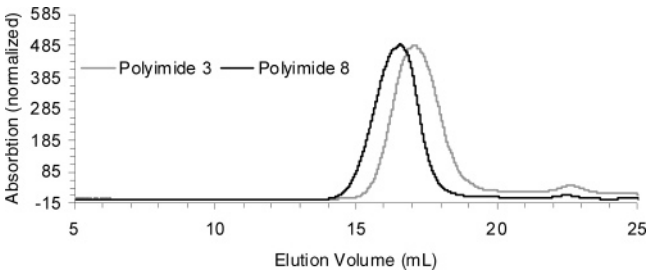

Figure 3. SEC trace showing shorter retention time (i.e., higher molecular weight) of POSS-functionalized polyimide **8** compared to retention of the corresponding nonfunctionalized polyimide **3**.

Analysis of the functionalized polyimides **6**−**9** by SEC is consistent with attachment of the POSS molecule, and there appears to be no evidence of cross-linking in the attachment chemistry. A typical set of SEC data is shown for polyimides **3** and **8** in Figure 3. The POSS-containing polyimide **8**, after two chemical reaction steps and two precipitations, shows by SEC essentially the same polydispersity as the starting polyimide **3**. Notably, the POSS-modified polymers show very good solubility in THF, chloroform, and dichloromethane; however, we were quite surprised when they showed solubility in diethyl ether!

Scheme 1

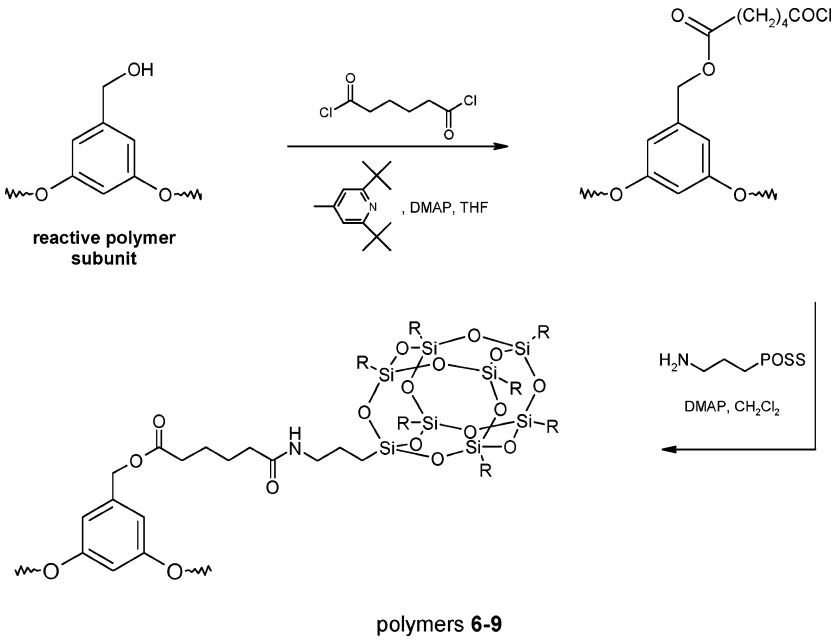

In addition to the pendant POSS examples shown above, it is desirable to have a multicomponent system that integrates a thermally curable side chain in addition to POSS. We selected two very different types of cross-linking groups to explore the merit of this approach with the new pendant POSS-polyimides. A cyanate ester group is selected on the basis of excellent thermal stability of the triazine that is formed upon reaction and methyl methacrylate on the basis of the wide array of curing reactions and initiators available.

Selective functionalization of the phenolic group in the commercially available 2-(4-hydroxyphenyl)ethanol is achieved in high yield and thus produced the hydroxyl-functionalized cyanate ester **10** (Scheme 2). The solvent choice is critical for minimizing formation of diethyl cyanamide, which is a byproduct that accompanies cyanate ester formation when performed in solvents such as THF, acetone, and dichloromethane (via the von Braun reaction). We find diethyl ether is the solvent of choice when synthesizing cyanate esters.

Scheme 2

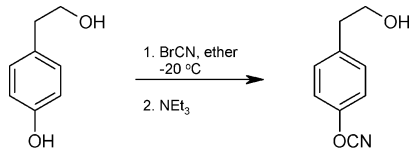

10

Employing the same polymer modification/attachment chemistry on polymer **5**, we find treatment of the pendant acid chloride intermediate polymer with a dichloromethane solution containing cyanate ester **10** and 3-aminopropyl-*i*-butylPOSS is successful in generating a multifunctional material with a final Si_8O_{12} content of 8 wt % and ~0.22 mequiv of −OCN per gram of polymer (Scheme 3).

Analogous to the example utilizing a cyanate ester-functionalized alcohol **10**, we can introduce a controlled amount of 2-hydroxyethyl methacrylate (HEMA) and POSS to polyimides **3** and **4** (Scheme 4) to afford the multifunctional polyimides **12** and **13**, respectively. A POSS to HEMA molar ratio of 4:1 is used, yielding a final Si_8O_{12} content of ~12.5 wt % for both polymers **12** and **13**.

Analysis of the multifunctional POSS polymers by ^{1}H NMR spectroscopy indicates that the pendant functional groups are present in the appropriate ratios. Thermally cured films of polyimide **12** were too brittle to warrant further analysis. On the other hand, polyimide **13** that is made with the nonfluorinated alkyldiamine RF-24 does produce high-quality free-standing films. We find that thin films (~25 μm) of polymers **6**−**9** and **11**−**13** can be aerosol sprayed onto Kapton H with good adhesion. This ability to coat and adhere to other polymeric materials is useful for a number of future potential applications.

Thermal Analysis and Curing Kinetics for the POSS-Polyimides. In Figure 4 we show in graphical terms the change in T_g as a function of POSS loading (as wt %) for polyimides **6**−**9**. The POSS cage occupies a significant volume as a side group and additionally should demonstrate a relative ease of rotational motion based on the flexible connections of the POSS cages to the polyimide backbones. Although the POSS cage itself is quite a rigid structure, the seven isobutyl groups provide a large number of degrees of conformational freedom. These factors increase the overall free volume in the bulk, thereby decreasing the ability of the polyimide chains to pack in an efficient manner. The reduction in T_g upon POSS modification is likely explained by a combination of these structural characteristics. Polyimide **6**, containing the least amount of POSS after modification (~8 wt % Si_8O_{12}), exhibits the lowest reduction in glass transition temperature. The relatively low T_g

Scheme 3

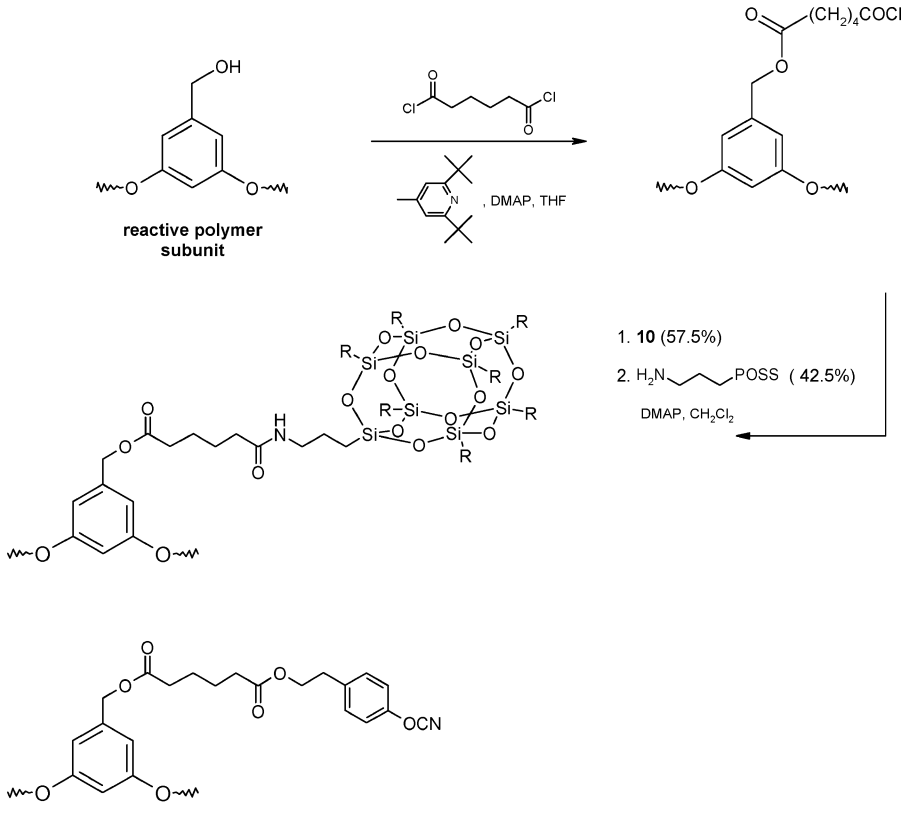

11

Scheme 4

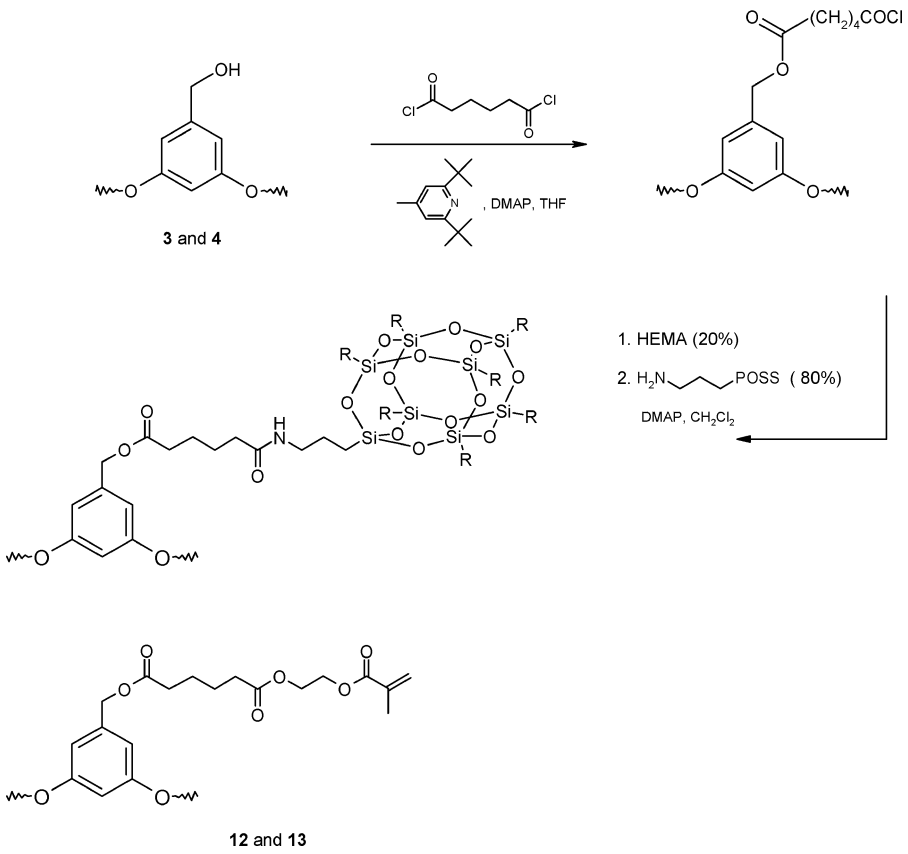

of polyimide **7** most likely results from the inclusion of the flexible group 1,5-diaminopentane within the polymer backbone. Last, polyimides **8** and **9** exhibit nearly identical and relatively high T_g's due to the same level of POSS attachment and the rigid nature of their polymer backbones.

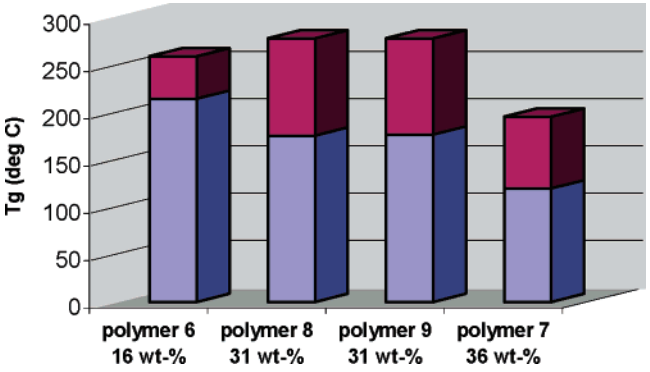

Figure 4. Comparison of pre- and postmodification T_g's for polymers **1**−**4** (total bar height, premodified) and **6**−**9** (lightly shaded bar, post modified). Vertical axis is T_g in °C.

Qualitative observations of the mechanical properties of the fabricated films revealed that the ability to cross-link the polyimide chains during the baking process resulted in dramatic improvements in fracture resistance in comparison with those polyimides devoid of reactive functionalities. With this realization in mind, it is useful to characterize the reaction kinetics of the curable polyimides. Typically thermal curing of these types of materials does not generate sufficient energy quantities for detection by DSC. Hence, it is necessary to execute kinetic analyses through an alternative method. The application of the DiBenedetto equation,[13−17] modified for highly cross-linked networks, provides a means of relating observed T_g's to extent of reaction:

$$\frac{T_g - T_{g0}}{T_{g\infty} - T_{g0}} = \frac{\lambda x}{1 - (1 - \lambda)x}$$

where T_g, T_{g0}, $T_{g\infty}$, λ, and x represent the glass transition temperature of the sample, the glass transition temperature of fresh uncured material, the glass transition temperature of the fully cured material, the ratio of the isobaric heat capacity of a fully cured model compound to that of an uncured model compound, and the extent of reaction (i.e., $C_t/C_0 = 1 - x$), respectively. The value of λ (=0.69) used in the present study was taken from the work of Scola and co-workers.[18]

For both **11** and **13** elevating the cure temperature results in an increase for the observed ultimate glass transition temperature achievable. Hence, the ultimate glass transition temperatures achieved by curing at 290 °C are used in the calculations for $T_{g\infty}$ (251 °C for **11** and **13**). Precure T_g's of 196 and 190 °C for **11** and **13**, respectively, are applied as T_{g0} in the DiBenedetto equation.

Thermal cycling of polyimides **11** and **13** after segmental isothermal cure (30 min blocks) rendered T_g data as a function of total cure time. Thus, a series of experiments were run for isothermal aging at temperatures between 230 and 290 °C. The acquired T_g's were then utilized in the Dibenedetto equation to afford a calculated extent of reaction as a function of curing time. The rate plots at the various temperatures were then analyzed using a first-order kinetic rate law. This analysis produced reaction rate constants for the cross-linking reaction at each temperature. These data are presented in the Arrhenius plot shown in Figure 5, and the kinetic parameters are summarized in Table 2.

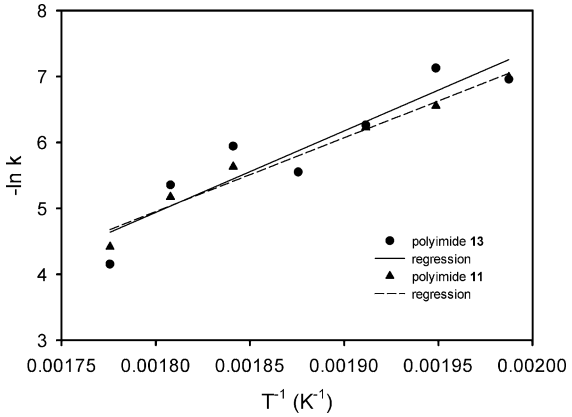

Figure 5. Arrhenius plot for the thermal curing of polyimides **11** and **13** with linear regression.

Table 2. Calculated Arrhenius and Eyring Parameters of Curing for Polyimides 11 and 13

	polymer **11**	polymer **13**
Arrhenius R^2	0.97	0.86
E_a (kJ/mol)	93	103
A (min^{-1})	3.8×10^6	3.3×10^7
Eyring R^2	0.97	0.84
H_{act} (kJ/mol)	88	98
S_{act} (J/kmol)	−132	−114

A fairly accurate fit is obtained using the first-order rate law for polyimides; however, deviations from linearity are most prominent at both low and high curing temperatures. The calculated activation energies, E_a, are statistically similar despite the difference in the type of reactive groups present in polyimide **11** over **13**. The activation energies obtained and the significant negative values for the activation entropies for both materials are consistent with a cycloaddition/polymerization reaction.

We have briefly explored the relative thermal stability for selected polymers using thermogravimetic analysis (TGA). Shown in Figure 6 are the TGA curves for polyimides **6**, **11**, and **13** (under air and nitrogen), and a summary of key aspects to the TGA plots can be found in Table 3.

Polyimide **13** demonstrated a different degradation profile than the others in that two maximum mass loss rates were observed. This is an interesting observation since this particular polyimide is cross-linked via HEMA groups. In reference to the chemical architectures of the polyimide backbones, although the HEMA cross-links represent additional bonds to be cleaved during the thermal degradation process, these particular cross-links may indeed be much less stable than the remainder of the segments and may contribute to the significantly earlier mass loss events observed in the plot. Uncurable polyimide **6** performed poorly in comparison with the cross-linked materials in terms of char yield, a likely result of the high loading level of aliphatic RF-24 in the polymer backbone. Polyimide **11** exhibited the best overall thermal stability due to its slightly lower loading level of RF-24 but more importantly its greater number of cross-links, which are thermally stable triazine rings formed through the reaction of the cyanate ester groups. Polyimide **13** suffers early mass losses in an oxygen-containing

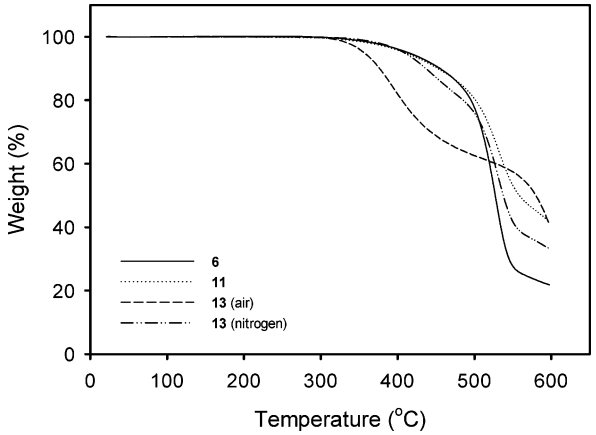

Figure 6. Graph of TGA curves for polyimides **6**, **11**, and **13** demonstrating mass loss of materials at elevated temperatures. A heating ramp rate of 10 °C/min is employed for runs.

Figure 7. Photograph of the ONR symbol (actual size 1.5 in. × 0.75 in.) taken through a thick film (∼50 μm) of polymer **7** supported on a glass slide. The film was doctor-bladed from a 20 wt % solution of cyclohexanone.

environment but exhibits a relatively high char yield due to the silicon component. The materials overall demonstrate thermal stability similar to other polyimides that contain the inorganic hybrid POSS cages.[19]

Film Processing and Atomic Oxygen Resistance Studies. Typical for all POSS-functionalized polymers produced in this study, polyimide **7** shows good solubility in a number of organic solvents, most likely as a result of the presence of the seven isobutyl substituents of POSS and the presence of the flexible alkyl spacer 1,5-diaminopentane in the polyimide backbone. Thick films (∼70 μm) of this material can be cast from 20 wt % solutions in cyclohexanone. The films appear essentially transparent and show only a slight brown coloration (Figure 7). This polymer provides an example of very high POSS loading (∼36 wt % POSS, ∼17 wt % Si_8O_{12}) while maintaining excellent film qualities.

Upon solvent-casting **9** (2 mil, 31 wt % POSS, ∼15 wt % Si_8O_{12}) a thin transparent free-standing film was obtained. The sample was exposed to an atomic oxygen beam using an apparatus and conditions published previously.[10] A Kapton H film is run concurrently in the chamber to provide an accurate and instant measure for the degree of stabilization (or passivation) toward chemical degradation. In addition, a mask is placed over the samples to provide a very detailed 3-dimensional architecture and greatly assists in measuring the physical loss of material in the exposed areas. Data from the AO exposure of polymer **9** show the new POSS-modified polyimide experi-

Table 3. Thermogravimetric Mass Loss Data for Polymers 6, 11, and 13

sample ID	5% mass loss temp (°C)	max rate temp 1 (°C)	max rate 1 (%/min)	max rate temp 2 (°C)	max rate 2 (%/min)	char yield at 600 °C (%)
6	414	528	14	n/a	n/a	22
11	410	530	7	n/a	n/a	42
13 (air)	356	393	4	593	6	41
13 (nitrogen)	409	439	2	534	9	33

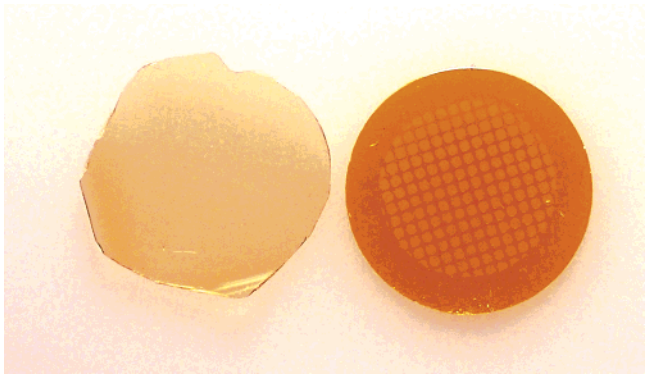

Figure 8. Photograph of polymer **9** (left) and the Kapton H standard (right) after side-by-side AO exposure.

ences no detectable degradation when exposed to atomic oxygen relative to Kapton H (the latter erodes ~11−12 μm for this amount of AO exposure). Typically, once the mask is removed from an AO exposed sample, a vivid pattern of the grid can be seen. A very unique feature for polymer **9** is that no pattern is detectable after mask removal and the films remain transparent (Figure 8).

Concluding Remarks. We have presented a facile route for the covalent attachment of a commercially available POSS unit to a variety of polyimide backbones. Furthermore, during the attachment chemistry a reactive cross-linking group can be added concomitant with POSS and thus generate a thermally curable and easily processed coating material. The POSS-modified polyimides prepared in this study have a wide range of T_g's (120−215 °C) and can possess a significant level of fluorine content with no apparent phase separation. By thermal curing reactions we can prepare POSS-polyimides that remain optically clear, show good solvent resistance, and develop a final T_g of 250 °C that is close to the T_g of the unmodified backbone. A 31 wt % POSS (15 wt % Si_8O_{12}) content material was tested for AO resistance and found to show exceptionally good characteristics with no detectable erosion relative to Kapton H.

Experimental Section

General Synthetic Methods. All manipulations of compounds and solvents were carried out using standard Schlenk techniques. 1-Methyl-2-pyrrolidinone (NMP), dichloromethane, tetrahydrofuran (THF), and ether solvents were purchased as the anhydrous grade and inhibitor-free from Aldrich and used as received. ^{1}H and ^{13}C NMR measurements were performed using a Bruker AC 200 or Bruker 400 MHz instrument. ^{1}H and ^{13}C NMR chemical shifts are reported versus the deuterated solvent peak (solvent, ^{1}H, ^{13}C: $CDCl_3$, δ 7.25 ppm, δ 77.0 ppm). Phthalic anhydride, 1,5-pentanediamine, 4-*tert*-butylaniline, adipoyl chloride, 4-(dimethylamino)pyridine (DMAP), 2,6-di-*tert*-butyl-4-methylpyridine, triethylamine, cyanogen bromide, 2-(4-hydroxyphenyl)ethanol, and 2-hydroxyethyl methacrylate were purchased from Aldrich Chemical Co. and used as received. 4,4′-(Hexafluoroisopropylidene)-diphthalic anhydride (6-FDA) and 2,2-bis(4-aminophenyl)hexafluoropropane were purchased from CHRISKEV Co. and used as received. The 2,2′-dimethyl-4,4′-methylenebis(cyclohexylamine) (RF-24) was purchased from Resin Formulators, and the 3-aminopropylhepta(*i*-butyl)POSS was purchased from Hybrid Plastics; both were used as received. Elemental analyses were performed at Atlantic Microlab, Inc., Norcross, GA.

Film Preparation. Films utilized in erosion testing through atomic oxygen exposure were prepared by dissolving the desired polyimide in cyclohexanone at a solute concentration of 12.5 wt %. The solutions were subsequently purified in a clean room environment through 5 μm syringe driven filter units. Free-standing Kapton H film substrates were coated with the resultant solutions by either conventional blade casting or spray coating using a household spraying device at minimal gas pressures. The coated films were baked or cured under an inert nitrogen atmosphere according to the appropriate protocol (2 h at 70 °C, 1 h at 200 °C, and then 4 h at 250 °C). Final target film thicknesses of 25−50 μm for AO testing were measured vertically using a Dektak profilometer.

Thermal Analysis Measurements and Techniques. Differential scanning calorimetry (DSC): Glass transition temperature (T_g) measurements for all of the polyimides, in addition to reaction kinetics studies for the curable polyimides, were conducted on a TA Instruments Q Series 10 calorimeter. Glass transition temperatures were obtained by analysis of dynamic temperature sweeps of 3−5 mg samples at a heating rate of 20 °C/min slightly beyond the observed inflection, followed by cooling to 50 °C and reheating again at a rate of 10 °C/min to obtain the desired T_g. Influences from sample repositioning and volatile release are eliminated through implementation of this technique. Isothermal curing data for the curable polyimides were acquired through thermal cycling and observance of T_g progression by holding the sample at the isothermal curing temperature for a 30 min period, followed by cooling to 70 °C at a rate of 5 °C/min, and then heating back to the curing temperature at a rate of 10 °C/min where the progressed T_g was witnessed. This procedure was followed until cessation of T_g movement was observed. Thermogravimetric analysis (TGA) was performed using a TA Instruments Hi-Res TGA 2950 thermogravimetic analyzer. The samples (2−3 mg) were heated in either nitrogen (30 mL/min) or air (30 mL/min) atmospheres from ambient temperature to 600 °C at a heating rate of 10 °C/min.

General Procedure for Preparation of CH_2OH-Functionalized Polyimide. A typical procedure is as follows: A Schlenk flask was charged with 3,5-bis(4-aminophenoxy)-1-hydroxymethylbenzene (1.000 g, 3.008 mmol), RF-24 (4.064 g, 17.045 mmol), and NMP (70 mL). When the solution had become homogeneous, 6-FDA (8.730 g, 19.651 mmol) and phthalic anhydride (0.119 g, 0.802 mmol, 2 mol % end-cap) were added in one portion. The mixture was stirred at ambient temperature for 16 h then fitted with a reflux condenser and immersed in an oil bath heated at 180 °C for 6 h. The reaction vessel was removed from the oil bath, allowed to spontaneously cool for 30 min, and then poured into a flask containing vigorously stirred methanol (1.5 L). Vigorous stirring of the methanol was maintained during the entire precipitation process. The precipitated polyimide was collected on a 600 mL medium porosity glass frit, washed with methanol (~1.5 L), and then dried under reduced pressure for 12 h at 70 °C. This gave CH_2OH-functionalized polyimide **1** (11.85 g, 90%, M_n ~ 4000, polydispersity 2.2, T_g 260 °C) as an off-white powder. ^{1}H NMR ($CDCl_3$): δ 8.15−7.55 (overlapping m, aromatic H's), 7.38 (d, J = 8.1 Hz, 4H), 7.14 (d, J = 8.2 Hz, 4H), 6.84 (s, 2H), 6.73 (s, 1H), 4.67, (s, 2H, CH_2OH), 4.45−4.13 (br m), 3.85−3.56 (br m), 2.65−0.50 (br overlapping m). Selected ^{13}C NMR ($CDCl_3$) signals: δ 167.7, 167.5, 166.4, 166.3, 158.2, 156.9, 138.9, 135.7, 132.8 (br), 128.3, 125.6 (br), 123.6 (br), 122.2, 119.6, 112.8, 109.7, 65.3 (br, CH_2OH), 57.8, 44.4 (br), 41.8 (br), 34.0 (br), 33.6 (br), 32.9 (br), 29.8, 19.4, 19.2. Anal. Calcd for **1**: C, 63.22; H, 4.64. Found: C, 61.85; H, 4.67. Polyimides **2**, **3**, **4**, and **5** were produced in a similar manner utilizing the appropriate monomers, and selected data are presented below:

Polymer 2 (24.0 g, 93%, M_n ~ 10 000, polydispersity 2.1, T_g 196 °C). ^{1}H NMR ($CDCl_3$): δ 8.15−7.65 (overlapping m, aromatic H's), 7.38 (d, J = 7.8 Hz, 4H), 7.13 (d, J = 7.5 Hz, 4H), 6.83 (s, 2H), 6.72 (s, 1H), 4.65 (s, 2H, CH_2OH), 3.69 (br s, 4H), 2.91 (br s), 1.72 (br s, 4H), 1.41 (br s, 2H). Selected ^{13}C NMR ($CDCl_3$) signals: δ 167.4, 167.3, 166.4, 166.3, 158.3, 156.9, 145.0, 139.5, 138.9, 138.8, 136.2, 135.7, 134.7, 134.1, 133.2−132.3 (br aromatic signals), 128.3, 126.6, 125.6, 125.0, 124.3, 124.0, 123.7, 123.4, 122.2, 119.6, 112.7, 109.7, 64.6 (CH_2OH), 38.3, 28.2, 24.3. Anal. Calcd for **2**: C, 59.93; H, 3.03. Found: C, 59.32; H, 3.06.

Polymer 3 (23.6 g, 80%, M_n ~ 9500, polydispersity 1.8, T_g 279 °C). ^{1}H NMR ($CDCl_3$): δ 8.11−7.77 (overlapping m, aromatic

H's), 7.62−7.48 (overlapping m, aromatic H's), 7.37 (br d, 4H), 7.13 (br d, 4H), 6.83 (br s, 2H), 6.71 (br s, 1H), 4.64 (br s, 2H, CH_2OH), 3.19 (br s, 1H, OH). Selected ^{13}C NMR ($CDCl_3$) signals: δ 166.4, 166.2, 166.0, 165.8, 158.2, 156.9, 144.9, 139.6, 139.3, 136.4, 136.2, 134.9, 134.7, 133.1−132.5 (br aromatic signals), 131.4, 128.3, 126.6, 126.1, 125.7, 125.6, 125.0, 124.6, 124.4, 124.2, 124.0, 122.2, 119.6, 112.8, 109.7, 64.6. Anal. Calcd for **3**: C, 58.37; H, 2.28. Found: C, 58.19; H, 2.34.

Polymer 4 (18.3 g, 78%, $M_n \sim 4300$, polydispersity 1.9, T_g 279 °C). ^1H NMR ($CDCl_3$): δ 8.02−7.65 (overlapping m, aromatic H's), 7.46−7.37 (m, 4H), 7.20−7.13 (m, 4H), 6.84 (s, 2H), 7.67 (br s, 1H), 4.66 (s, 2H, CH_2OH), 4.37−4.15 (br m), 3.86−3.62 (br m), 2.55−0.42 (br overlapping m).

Polymer 5 (12.3 g, 87%, $M_n \sim 5500$, polydispersity 1.8, T_g 267 °C). ^1H NMR ($CDCl_3$): δ 8.15−7.60 (overlapping m, aromatic H's), 7.52 (d, $J = 7.8$ Hz), 7.45−7.29 (m, 4H), 7.21−7.04 (m, 4H), 6.84 (s, 2H), 6.72 (s, 1H), 4.65 (s, CH_2OH), 3.95−3.55 (br m), 2.65−0.50 (br overlapping m), 1.35 (s, 9H). Selected ^{13}C NMR ($CDCl_3$) signals: δ 167.7, 167.5, 166.44, 166.39, 166.3, 158.2, 156.9, 144.9, 139.5, 139.4, 138.8, 136.2, 135.7, 133.0−132.3 (br aromatic signals), 128.3, 126.6, 126.5, 126.2, 125.6, 125.0 (br), 124.3, 123.6 (br), 122.2, 119.6, 112.6, 109.7, 64.6 (CH_2OH), 57.8, 41.9, 34.0, 33.6, 32.9, 31.5, 29.8, 19.4, 19.2. Anal. Calcd for **5**: C, 62.95; H, 4.02. Found: C, 61.51; H, 4.06.

General Procedure for the Modification of Polyimide-CH_2OH with a Diacid Chloride. A typical procedure is as follows: A THF solution (20 mL) containing polyimide **1** (2.0 g, 0.457 mequiv of OH/g), 2,6-di-*tert*-butyl-4-methylpyridine (400 mg, 1.94 mmol), and DMAP (40 mg, 0.33 mmol) was treated with adipoyl chloride (2.5 mL, 17.14 mmol). Some precipitate was seen to form over the reaction period of 18 h, after which time the mixture was filtered through a plug of Celite (1 × 2.5 cm) into a rapidly stirred solution of ether (400 mL). The polymer was collected by filtration and washed with ether (2 × 150 mL), taking care to protect the solution and polymer from air, and then dried under reduced pressure (0.2 Torr) for 30 min to afford 1.4 g (∼68%) of acid chloride modified polyimide **1** containing ∼5 wt % residual ether. The polymer is used immediately for the next reaction without further purification. Polyimides **2**, **3**, **4**, and **5** were functionalized in a similar manner and were utilized immediately after formation.

General Procedure for Attachment of POSS to Acid Chloride Functionalized Polyimide. A typical procedure is as follows: The acid chloride functionalized polyimide **1** (1.4 g) was dissolved in dichloromethane (35 mL) and then treated with 3-aminopropyl-isobutyl-POSS (287 mg, 0.329 mmol). This mixture was stirred for 5 min, and then in one portion DMAP (100 mg, 0.52 mmol) was added. The mixture was allowed to react with stirring for 2 h at ambient temperature, concentrated to ∼20 mL, and added to a rapidly stirred solution of methanol (400 mL). The resulting polymer was collected on a 150 mL medium-porosity glass frit, washed with methanol (2 × 150 mL), and then dried under reduced pressure at ∼45 °C (∼0.2 Torr) for 24 h to afford POSS-functionalized polyimide **6** (1.5 g, 94%, $M_n \sim 11\,700$, polydispersity 2.0, T_g 215 °C) as an off-white powder. ^1H NMR ($CDCl_3$): δ 8.22−7.50 (overlapping m, aromatic H's), 7.40 (d, $J = 8.3$ Hz, 4H), 7.16 (d, $J = 8.6$ Hz, 4H), 6.82 (br s, 2H), 6.75 (br s, 1H), 6.69 (m), 5.51 (br s), 5.07 (br s, 2H, CH_2OH), 4.61 (br s), 4.38−4.19 (br m), 3.92−3.73 (br m), 3.23−3.19 (m), 3.95−3.82 (br m), 2.62−0.57 (br overlapping m), 0.59 (d, $J = 6.6$ Hz, 14H). Anal. Calcd for **6**: C, 59.89; H, 5.24. Found: C, 59.04; H, 5.35. Polyimides **7**, **8**, and **9** were produced in a similar manner, and selected data are presented below:

Polymer 7 (830 mg, 86%, $M_n \sim 10\,000$, polydispersity 1.8, T_g 120 °C). ^1H NMR ($CDCl_3$): δ 8.01−7.72 (overlapping m, aromatic H's), 7.39 (d, $J = 8.5$ Hz, 4H), 7.14 (d, $J = 8.6$ Hz, 4H), 5.51 (br s, 1H, NH), 5.05 (s, 2H, CH_2OH), 3.75−3.57 (br m), 3.25−3.12 (m), 2.41−1.19 (br overlapping m), 0.93 (br d, 42H), 0.58 (d, $J = 7.0$ Hz, 14H). Anal. Calcd for **7**: C, 54.01; H, 4.97. Found: C, 53.33; H, 4.98.

Polymer 8 (2.2 g, 85%, $M_n \sim 9000$, polydispersity 1.8, T_g 176 °C). ^1H NMR ($CDCl_3$): δ 8.13−7.72 (overlapping m, aromatic H's), 7.63−7.48 (m, aromatic H's), 7.40 (d, $J = 8.3$ Hz, 4H), 7.14 (d, $J = 8.3$ Hz, 4H), 5.51 (br s, 1H, NH), 5.06 (s, 2H, CH_2OH), 3.27−3.16 (m), 2.41−2.09 (overlapping m), 1.88−1.63 (overlapping m), 0.93 (br d, 42H), 0.58 (d, $J = 7.0$ Hz, 14H). Anal. Calcd for **8**: C, 53.73; H, 4.25. Found: C, 53.53; H, 4.33.

Polymer 9 (880 mg, 63%, $M_n \sim 11\,500$, polydispersity 2.9, T_g 177 °C). ^1H NMR ($CDCl_3$): δ 8.05−7.62 (overlapping m, aromatic H's), 7.40 (d, $J = 7.5$ Hz, 4H), 7.15 (d, $J = 7.5$ Hz, 4H), 6.81 (br s, 2H), 6.74 (br s, 1H), 5.51 (br s, 1H, NH), 5.06 (br s, 2H, CH_2-OH), 4.35−4.19 (br m), 3.83−3.12 (m), 3.28−3.09 (m), 2.45−0.79 (br overlapping m), 0.58 (d, $J = 6.9$ Hz, 14H).

Preparation of 2-(4-Cyanatophenyl)ethanol (10). A chilled (−20 °C) ether (55 mL) solution containing 2-(4-hydroxyphenyl)-ethanol (1.50 g, 10.9 mmol) and cyanogen bromide (1.49 g, 14.1 mmol) was treated dropwise with triethylamine (1.51 mL, 10.9 mmol). A white precipitate was seen to form immediately, and after 30 min the solid was removed by filtration on a medium-porosity glass frit and washed with ether (150 mL). The filtrate was washed with water (2 × 100 mL), dried ($MgSO_4$), filtered, and concentrated under reduced pressure to yield **10** (1.4 g, 79%) as a clear colorless viscous oil. ^1H NMR ($CDCl_3$): δ 7.34−7.20 (m, 4H), 3.86 (appt. q, $J = \sim 6.5$ Hz 2H), 2.88 (t, $J = 6.5$ Hz, 2H), 1.46 (t, $J = 5.5$ Hz, 1H, OH); ^{13}C NMR ($CDCl_3$) δ 151.5 (aromatic C−O), 137.7 (aromatic C), 130.9, 115.3 (aromatic CH's), 108.8 (OCN), 63.3 (CH_2OH), 38.2 (CH_2).

Attachment of POSS and 2-(4-Cyanatophenyl)ethanol (10) to Acid Chloride-Functionalized Polyimide (5). Acid chloride-functionalized polyimide **5** (3.4 g) was dissolved in dichloromethane (100 mL) and then treated with a 100 mg/mL dichloromethane solution of 2-(4-cyanatophenyl)ethanol (**10**) (176 mg, 1.078 mmol) and 3-aminopropylisobutyl-POSS (702 mg, 0.80 mmol). DMAP (340 mg, 2.78 mmol) was immediately added, and the mixture stirred for 2 h at ambient temperature. The mixture was then concentrated to ∼50 mL and added to a rapidly stirred solution of methanol (800 mL). The resulting polymer was collected on a 300 mL medium-porosity glass frit, washed with methanol (2 × 250 mL), and then dried under reduced pressure at ∼45 °C (∼0.2 Torr) for several hours to give POSS/cyanate ester-functionalized polyimide **11** (3.4 g, 81%, $M_n \sim 7000$, polydispersity 1.8, precure T_g 196 °C) as an off-white powder. ^1H NMR ($CDCl_3$): δ 8.17−7.49 (overlapping m, aromatic H's), 7.39 (d, $J = 8.2$ Hz, 4H), 7.14 (d, $J = 8.2$ Hz, 4H), 6.80−6.65 (overlapping signals), 5.01 (br s, 1H, NH), 5.06 (br s, 2H, CH_2OH), 4.25−4.4.19 (m, 2H). 3.83−3.61 (br m), 3.23−3.15 (m), 2.99−2.73 (br m), 2.48−0.80 (br overlapping m), 0.58 (d, $J = 6.8$ Hz, 14H). Anal. Calcd for **11**: C, 59.92; H, 4.83. Found: C, 59.43; H, 4.88.

Attachment of POSS and HEMA to Acid Chloride-Functionalized Polyimide (3). Acid chloride-functionalized polyimide **3** (2.1 g) was dissolved in dichloromethane (50 mL) and then treated with HEMA (53 mg, 0.41 mmol, 0.4 equiv) and 3-aminopropyl-isobutyl-POSS (710 mg, 0.81 mmol, 0.8 equiv). DMAP (200 mg, 1.6 mmol) was immediately added, and the mixture was stirred for 6 h at ambient temperature. The mixture was then concentrated to ∼20 mL and added to a rapidly stirred solution of methanol (400 mL). The resulting polymer was collected on a 150 mL medium-porosity glass frit, washed with methanol (2 × 100 mL), and then dried under reduced pressure at ∼45 °C (∼0.2 Torr) for several hours to give POSS/HEMA-functionalized polyimide **12** (2.25 g, 83%, $M_n \sim 6000$, polydispersity 1.5, precure T_g 167 °C). ^1H NMR ($CDCl_3$): δ 8.08−7.78 (overlapping m, aromatic H's), 7.61−7.50 (m, aromatic H's), 7.40 (d, $J = 8.7$ Hz, 4H), 7.14 (d, $J = 8.7$ Hz, 4H), 6.81 (br s, 2H), 6.74 (br s, 1H), 6.19 (br s, olefinic H), 5.56 (br s, 2H, olefinic H and NH), 5.06 (br s, 2H, CH_2OH), 4.35−4.28 (m), 3.34−3.12 (m, 2H), 2.46−2.29 (br m), 2.24−2.06 (br m), 1.90−1.52 (overlapping m), 0.99−0.82 (m, 42H), 0.58 (d, $J = 7.0$ Hz, 14H). Anal. Calcd for **12**: C, 54.48; H, 4.02. Found: C, 54.35; H, 4.13.

Attachment of POSS and HEMA to Acid Chloride-Functionalized Polyimide (4). Acid chloride-functionalized polyimide **4** (1.9 g) was dissolved in dichloromethane (45 mL) and then treated with HEMA (43.7 mg, 0.34 mmol, 0.4 equiv) and 3-aminopropy-

lisobutyl-POSS (587 mg, 0.67 mmol, 0.8 equiv). DMAP (170 mg, 1.39 mmol) was immediately added, and the mixture stirred for 8 h at ambient temperature. The mixture was then concentrated to ~25 mL and added to a rapidly stirred solution of methanol (400 mL). The resulting polymer was collected on a 150 mL medium-porosity glass frit, washed with methanol (2 × 150 mL), and then dried under reduced pressure at ~45 °C (~0.2 Torr) for several hours to give POSS/HEMA-functionalized polymer **13** (1.97 g, 87%, $M_n \sim 11\,000$, polydispersity 2.1, precure T_g 190 °C). ^{1}H NMR ($CDCl_3$): δ 8.02−7.63 (overlapping m, aromatic H's), 7.40 (d, $J = 7.7$ Hz, 4H), 7.14 (d, $J = 7.5$ Hz, 4H), 6.92−6.75 (br overlapping s), 6.08 (br s, olefinic H), 5.52 (br s, 2H, olefinic H and NH), 5.06 (br s, 2H, CH_2OH), 4.31 (br s), 3.86−3.66 (br m), 3.28−3.12 (br m), 2. 42−0.66 (br overlapping m), 0.58 (d, $J = 6.6$ Hz, 14H). Anal. Calcd for **13**: C, 57.69; H, 5.26. Found: C, 56.37; H, 5.13.

Acknowledgment. DoD researchers acknowledge partial support of this work through ONR, AFOSR, and DARPA. We thank Ms. Vandana Vij and Mr. Dan Bliss for their technical assistance. B.J.P. and G.R.Y. acknowledge support from ASEE postdoctoral fellowships.

References and Notes

(1) Feher, F. J.; Newman, D. A.; Walzer, J. F. *J. Am. Chem. Soc.* **1989**, *111*, 1741 and references therein. Feher, F. J.; Budzichowski, T. A. *Polyhedron* **1995**, *14*, 3239−3253.

(2) For more general reviews see: Voronkov, M. G.; Lavrent'yev, V. I. *Top. Curr. Chem.* **1982**, *102*, 199−235. Baney, R. H.; Itoh, M.; Sakakibara, A.; Suzuki, T. *Chem. Rev.* **1995**, *95*, 1409−1430. Murugavel, R.; Voigt, A.; Walawalkar, M. G.; Roesky, H. W. *Chem. Rev.* **1996**, *96*, 2205−2236. Lichtenhan, J. In *Polymeric Materials Encyclopedia*; Salomone, J. C., Ed.; CRC Press: New York, 1996; Vol. 10, pp 7768−7777. Provatas, A.; Matisons, J. G. *Trends Polym. Sci.* **1997**, *5*, 327−333.

(3) A large of array of monofunctionalized POSS molecules is commercially available (Hybrid Plastics, Inc.). The primary synthetic route involves corner-capping a trisilanol POSS precursor (see: Feher, F. J.; Budzichowski, T. A.; Blanski, R. L.; Weller, K. J.; Ziller, J. W. *Organometallics* **1991**, *10*, 2526) with a functionalized $RSi(OMe)_3$ reagent (where R can contain a wide range of organic functionalities).

(4) For a compilation of papers that provide a broad overview of activity in the area of POSS materials see: *Inorganic Hybrid Materials*; Klein, L., De Guire, M., Lorraine, F., Mark, J., Eds.; MRS Symposium Series 576; Materials Research Society: Warrendale, PA 1999.

(5) For examples see: Zheng, L.; Waddon, R. J.; Farris, R. J.; Coughlin, E. B. *Macromolecules* **2002**, *35*, 2375. Jeoung, E.; Carrol, J. B.; Rotello, V. M. *Chem. Commun.* **2002**, 1510. Carroll, J. B.; Frankamp, B. L.; Srivastava, S.; Rotello, V. M. *Mater. Chem.* **2004**, *14*, 690−694 and references therein.

(6) Wright, M. E.; Schorzman, D. A.; Feher, F. J.; Jin, R.-Z. *Chem. Mater.* **2003**, *15*, 264−268.

(7) Laine, R. M. *J. Mater. Chem.* **2005**, *15*, 3725−3744 and references therein.

(8) Liang, K.; Toghiani, H.; Li, G.; Pittman, C. U., Jr. *J. Polym. Sci., Part A: Polym. Chem.* **2005**, *43*, 3887−3898 and references therein.

(9) Kawakami, Y.; Imae, I. *J. Mater. Chem.* **2005**, *15*, 4581−4583 and references therein.

(10) Brunsvold, A. L.; Minton, T. K.; Gouzman, I.; Grossman, E.; Gonzalez, R. *High Perform. Polym.* **2004**, *16*, 303−318 and references therein.

(11) Hoflund, G. B.; Gonzalez, R. I.; Phillips, S. H. *J. Adhes. Sci. Technol.* **2001**, *15*, 1199−1211. Gonzalez, R. I.; Phillips, S. H. *J. Spacecraft Rockets* **2000**, *37*, 463−467. Phillips, S. H.; Haddad, T. S.; Tomczak, S. J. *Curr. Opin. Solid State Mater. Sci.* **2004**, *8*, 21−29 and references therein.

(12) Wright, M. E.; Fallis, S.; Guenthner, A. J.; Baldwin, L. C. *Macromolecules* **2005**, *38*, 10014−10021.

(13) DiBenedetto, A. T. *J. Polym. Sci., Part B: Polym. Phys.* **1987**, *25*, 1949−1969.

(14) Pascault, J. P.; Williams, R. J. J. *J. Polym. Sci., Part B: Polym. Phys.* **1990**, *28*, 85−96.

(15) Hale, A.; Macosko, C. W.; Bair, H. E. *Macromolecules* **1991**, *24*, 2610−2621.

(16) Nielson, L. E. *J. Macromol. Sci., Rev. Macromol. Chem.* **1969**, *C3*, 69.

(17) Couchman, P. R. *Macromolecules* **1987**, *20*, 1712−1717.

(18) Fang, X.; Rogers, D. F.; Scola, D. A.; Stevens, M. P. *J. Polym. Sci., Part A: Polym. Chem.* **1998**, *36*, 461−470.

(19) For an example of a hyper-cross-linked material prepared from octa-(4-aminophenyl)POSS see: Tamaki, R.; Tanaka, Y.; Asuncion, M. Z.; Choi, J.; Laine, R. M. *J. Am. Chem. Soc.* **2001**, *123*, 12416−124417. See ref 6 in this paper for soluble polyimides that contained thermally curable end-caps. For a study on the thermal decomposition of POSS structures see: Fina, A.; Tabuani, D.; Carniato, F.; Frache, A.; Boccaleri, E.; Camino, G. *Thermochim. Acta* **2006** *440*, 36−42.

MA060372D